Histone Lysine Demethylase JARID1a Activates CLOCK-BMAL1 and Influences the Circadian Clock

ways that are not feasible offline, there are also important limitations. First, unlike laboratory studies, we have little data on conditions that are known to influence mood, including demographic and occupational backgrounds that may influence when and how much people sleep, the level and timing of environmental stress, susceptibility to affective contagion, and access to social support. Second, lexical analysis measures the expression of affect, not the experience. Cultural norms may regulate the appropriateness of affective expression at different times of the day or week. Because these norms are unlikely to be universal, the robust patterns we observed across diverse cultures (as well as across days of the week) give us confidence that affective expression is a reliable indicator of diurnal individual-level variations in affective state.

References and Notes

1. F. G. Ashby, V. V. Valentin, U. Turken, in *Emotional Cognition: From Brain to Behaviour*, S. Moore, M. Oaksford, Eds. (Benjamins, Amsterdam, 2002), pp. 245–287.
2. S. C. Segerstrom, S. E. Sephton, *Psychol. Sci.* **21**, 448 (2010).
3. C. Kirschbaum, D. H. Hellhammer, *Neuropsychobiology* **22**, 150 (1989).
4. A. A. Stone et al., *Emotion* **6**, 139 (2006).
5. J. R. Vittengl, C. S. Holt, *Motiv. Emot.* **22**, 255 (1998).
6. L. A. Clark, D. Watson, J. Leeka, *Motiv. Emot.* **13**, 205 (1989).
7. D. B. Boivin et al., *Arch. Gen. Psychiatry* **54**, 145 (1997).
8. B. P. Hasler, M. R. Mehl, R. R. Bootzin, S. Vazire, *J. Res. Pers.* **42**, 1537 (2008).
9. J. Henrich, S. J. Heine, A. Norenzayan, *Behav. Brain Sci.* **33**, 61 (2010).
10. N. Bolger, A. Davis, E. Rafaeli, *Annu. Rev. Psychol.* **54**, 579 (2003).
11. D. Lazer et al., *Science* **323**, 721 (2009).
12. J. Bollen, A. Pepe, H. Mao, in *International AAAI Conference on Weblogs and Social Media* (Barcelona, 2011).
13. B. O'Connor, R. Balasubramanyan, B. R. Routledge, N. A. Smith, in *International AAAI Conference on Weblogs and Social Media* (Washington, DC, 2010).
14. P. S. Dodds, C. M. Danforth, *J. Happiness Stud.* **11**, 441 (2010).
15. A. D. I. Kramer, in *Proceedings of the 2010 Annual Conference on Human Factors in Computing Systems* (CHI '10) (2010), pp. 287–290.
16. A. Mislove, S. Lehmann, Y. Ahn, J. Onnela, J. N. Rosenquist, www.ccs.neu.edu/home/amislove/twittermood/.
17. J. W. Pennebaker, M. E. Francis, R. J. Booth, *Linguistic Inquiry and Word Count (LIWC): LIWC2001* (Erlbaum, Mahwah, NJ, 2001).
18. E. O. Bantum, J. E. Owen, *Psychol. Assess.* **21**, 79 (2009).
19. See supporting material on *Science* Online.
20. S. Daan, D. G. M. Beersma, A. A. Borbély, *Am. J. Physiol.* **246**, R161 (1984).
21. Abu Dhabi Government Portal, Working Hours Policy, 2010; www.abudhabi.ae/.
22. R. W. Lam, R. D. Levitan, *J. Psychiatry Neurosci.* **25**, 469 (2000).
23. N. E. Rosenthal et al., *Arch. Gen. Psychiatry* **41**, 72 (1984).
24. M. Terman, J. S. Terman, in *Principles and Practice of Sleep Medicine*, M. H. Kryger, T. Roth, W. C. Dement, Eds. (Elsevier, Philadelphia, ed. 4, 2005), pp. 1424–1442.
25. W. C. Forsythe, E. J. Rykiel Jr., R. S. Stahl, H. Wu, R. M. Schoolfield, *Ecol. Modell.* **80**, 87 (1995).
26. G. Murray, N. B. Allen, J. Trinder, *Chronobiol. Int.* **18**, 875 (2001).
27. N. E. Rosenthal, *Winter Blues* (Guilford, New York, 2006).

Histone Lysine Demethylase JARID1a Activates CLOCK-BMAL1 and Influences the Circadian Clock

Luciano DiTacchio,[1] Hiep D. Le,[1] Christopher Vollmers,[1] Megumi Hatori,[1] Michael Witcher,[2] Julie Secombe,[3] Satchidananda Panda[1]*

In animals, circadian oscillators are based on a transcription-translation circuit that revolves around the transcription factors CLOCK and BMAL1. We found that the JumonjiC (JmjC) and ARID domain–containing histone lysine demethylase 1a (JARID1a) formed a complex with CLOCK-BMAL1, which was recruited to the *Per2* promoter. JARID1a increased histone acetylation by inhibiting histone deacetylase 1 function and enhanced transcription by CLOCK-BMAL1 in a demethylase-independent manner. Depletion of JARID1a in mammalian cells reduced *Per* promoter histone acetylation, dampened expression of canonical circadian genes, and shortened the period of circadian rhythms. *Drosophila* lines with reduced expression of the *Jarid1a* homolog, *lid*, had lowered *Per* expression and similarly altered circadian rhythms. JARID1a thus has a nonredundant role in circadian oscillator function.

To gain insight into the dynamics of chromatin modifications and the function of CLOCK-BMAL1 transcription factors in the circadian clock, we measured the state of two histone modifications that correlate with active transcription, acetylation of histone 3 (H3) lysine 9 (H3K9Ac), and trimethylation of H3 lysine 4 (H3K4me3) at the *Per2* promoter (*1*). In mouse liver, both modifications synchronously oscillated at the *Per2* gene promoter CLOCK-BMAL1 E2–binding site ("E-box") (*2*), with lowest amounts at circadian time (CT, the endogenous, free-running time) 3 hours after the onset of activity (CT3) and peak amounts at CT12 (Fig. 1A). The peaks of histone modification were followed by those of *Per2* mRNA abundance. We also found BMAL1 abundance rhythms at the E-box, which reached a maximum at CT9 (Fig. 1B). Histone acetyltransferases (HATs) and histone deacetylases (HDACs) generate rhythms in histone acetylation and have important roles in circadian rhythms

(*3*, *4*). H3K4me3 modification at promoter regions correlates with transcriptional potential, which suggests that this mark helps maintain a transcriptionally poised state (*5*). Recently, the H3K4 methyltransferase MLL1 was shown to have a necessary role in CLOCK-BMAL1–dependent transcription (*6*).

We focused on a JumonjiC (JmjC) domain–containing H3K4me3 demethylase family with four mammalian and one insect gene members (fig. S1). In murine liver chromatin, JARID1a was enriched at the *Per2* E-box, and its profile at this site coincided with that of BMAL1 (Fig. 1B). *Jarid1a* expression in liver did not show robust oscillations (fig. S2), which suggested that recruitment of JARID1a to the *Per2* promoter might be mediated by the circadian machinery. Indeed, JARID1a recruitment to the *Per2* promoter E-box but not at a non–CLOCK-BMAL1 JARID1a target is reduced in $Bmal1^{-/-}$ cells (Fig. 1C and fig. S17A). Consistently, immunoprecipitation of endogenous CLOCK or BMAL1 from nuclear extracts copurified with endogenous JARID1a (Fig. 1D). Similarly, CLOCK and BMAL1 associated with immunoprecipitated JARID1a (fig. S3). Overexpression of JARID1a enhanced CLOCK-BMAL1–mediated transcription from *Per2* (Fig. 1E) and *Per1* (fig. S4A) promoters in a dose-dependent manner but failed to coactivate expression from an unrelated (E74-Luc) reporter (fig. S4D). Furthermore, coactivation of CLOCK-BMAL1 by JARID1a did not require its histone demethylase activity, as JARID1a mutants that carry a loss-of-function mutation (H483A, in which Ala replaces His[483]) (*7*) or that lack the JmjC domain enhanced CLOCK-BMAL1 activity, reversed

[1]Regulatory Biology Laboratory, Salk Institute for Biological Studies, La Jolla, CA 92037, USA. [2]Department of Oncology, McGill University, Montreal, Quebec H2W 1S6, Canada. [3]Department of Genetics, Albert Einstein College of Medicine, 1300 Morris Park Avenue, Bronx, NY 10461, USA.

*To whom correspondence should be addressed. E-mail: satchin@salk.edu

HDAC1 repression, and increased acetylation amounts at the *Per2* E-box (Fig. 1F and figs. S4B, S4C, and S5).

In contrast, JARID1b and JARID1c repressed CLOCK-BMAL1–mediated activation of *Per2* transcription (fig. S6, A and B). Accordingly, overexpression of JARID1b and JARID1c, but not JARID1a, reduced H3K4me3 modification at the *Per2* promoter (fig. S6C). Overall, these

results suggest that JARID1a enhances CLOCK-BMAL1 activation of the *Per2* promoter, whereas JARID1b and JARID1c might function to reverse its H3K4me3 levels during the repression phase of *Per* transcription.

To test whether JARID1a has a nonredundant role in the cell-autonomous oscillator, we stably transfected a *Per2:Luciferase* (*Per2:Luc*) reporter into fibroblasts derived from either *Jarid1a*$^{+/+}$

(wild type; WT) or *Jarid1a*$^{-/-}$ (knockout, KO) mice (7) and monitored circadian rhythms in *Per2:Luc* luminescence. In cell populations (Fig. 2A and fig. S7A) and single cells (fig. S8), *Per2* transcriptional rhythms in a *Jarid1a*$^{-/-}$ genetic background showed a significantly shorter period than those of WT controls [WT = 23.7 ± 0.2 hours, KO = 22.4 ± 0.3 hours, $P = 6.68 \times 10^{-8}$, $n = 10$ each genotype, one-way analysis of variance

Fig. 1. JARID1a coactivates CLOCK-BMAL1–mediated transcription of *Per* genes. (**A**) H3K4 trimethylation and H3K9 acetylation oscillations at the *Per2* promoter E-box in mouse liver shown alongside *Per2* mRNA expression (secondary y axis). Normalized average (+SEM, $n = 3$) of chromatin immunoprecipitations (ChIPs) performed with antibodies against H3K4me3 or H3K9Ac followed by QPCR analysis. Chromatin modifications shown as a percentage of total chromatin used (input) normalized to the corresponding lowest value (H3K4me3 = 0.27%, H3K9Ac = 0.25%) for ease of comparison. (**B**) Abundance of BMAL1 and JARID1a in mouse liver at the *Per2* promoter E-box and flanking regions. (**C**) Absence of JARID1a from the *Per2* promoter E-box in *Bmal1*$^{-/-}$ cells. (**D**) Association of endogenous JARID1a and CLOCK-BMAL1. Immunoprecipitates (IPs) obtained with the indicated antibodies from asynchronous U2OS (a human osteosarcoma cell line) nuclear extracts were immunoblotted (IB) with antibodies against JARID1a, CLOCK, BMAL1, or βACTIN. (**E**) Effect of JARID1a on CLOCK-BMAL1–dependent transcription from a *Per2:Luc* reporter. Luciferase activity (light counts) from HEK293T cells transiently expressing full-length JARID1a cDNA and *Per2:Luc* reporter construct are shown. (**F**) Wild-type (WT) or demethylase-mutant JARID1a H483A (MUT) rescues CLOCK-BMAL1 activation of a *Per2* reporter construct in *Jarid1a*$^{-/-}$ cells.
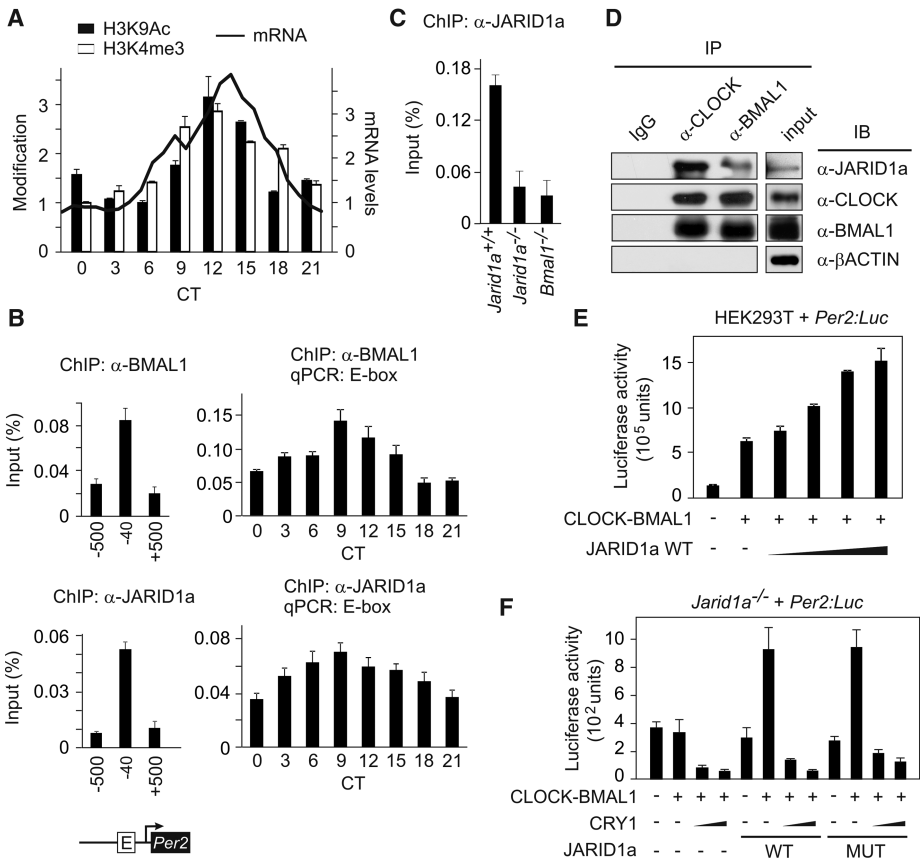
Fig. 2. JARID1a is required for normal circadian function. (**A**) Real-time bioluminescence from *Jarid1a*$^{+/+}$ (black) and *Jarid1a*$^{-/-}$ (red) mouse fibroblasts stably expressing a *Per2:Luc* construct. (Middle and right) Average period lengths (+SEM, $n = 10$) and amplitude estimates (***$P < 0.001$, two-tailed Student's *t* test). (**B**) *Per2*, *Cry1*, *Dbp*, and *SDF1* mRNA abundance in *Jarid1a*$^{+/+}$ cells (black) and *Jarid1a*$^{-/-}$ cells (red). Forty-eight hours after circadian synchronization, cells were collected at 3-hour intervals over the course of 24 hours, and the mRNA abundance was analyzed by reverse transcription (RT)–QPCR and normalized to that of *Gapdh*. Average normalized values (±SEM, $n = 3$) are plotted at various times after cell synchronization. (**C**) Representative real-time luminescence from U2OS cells stably expressing *Bmal1:Luc* and transfected with scrambled (S, black) or *Jarid1a* siRNA (red). Effects of different *Jarid1a* siRNA concentrations (10, 20, and 40 nM) on the endogenous *Jarid1a* mRNA abundance (average + SEM, $n = 3$) and period length (average + SEM, $n = 5$) relative to those of cells transfected with scrambled siRNA (40 nM). Representative results from at least three independent repetitions are shown.
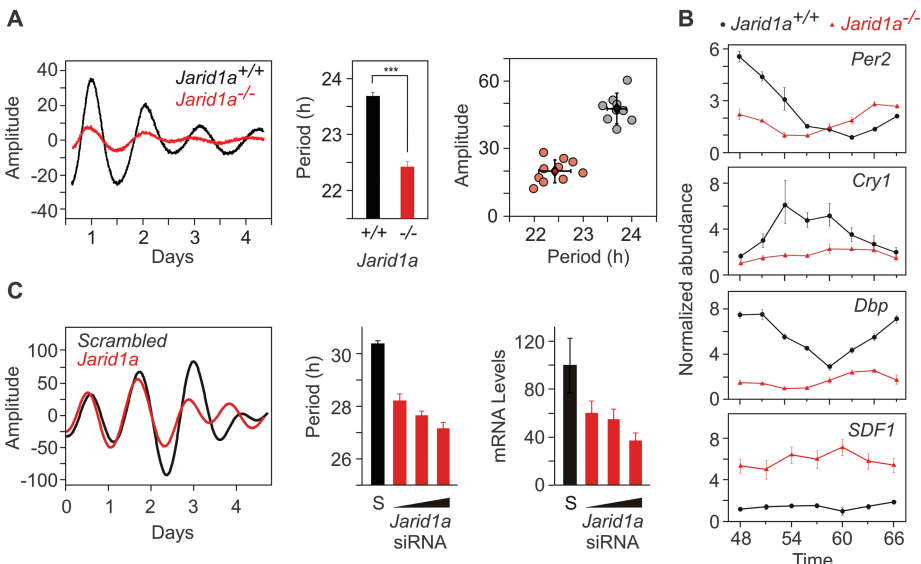
(ANOVA)] (Fig. 2A). Amounts of endogenous *Per2* transcript were also reduced and oscillated with a shorter period in *Jarid1a*$^{-/-}$ cells (Fig. 2B). Similarly, other CLOCK-BMAL1 targets were significantly reduced in *Jarid1a*$^{-/-}$ cells, and their rhythms were either absent or dampened (Fig. 2B and fig. S9). In contrast, abundance of *SDF1* mRNA, a repressive target of the histone demethylase (KDM) activity of JARID1a (7), was increased in *Jarid1a*$^{-/-}$ fibroblasts. Acute small interfering RNA (siRNA)–mediated depletion of *Jarid1a* mRNA also shortened circadian period length in a dose-dependent manner (Fig. 2C and fig. S7B). Conversely, transient transfection reconstitution of either wild-type or demethylase mutant JARID1a into *Jarid1a*$^{-/-}$ cells resulted in a circadian period lengthening (fig. S10). These results indicate that JARID1a has a nonredundant role in maintaining the normal periodicity of the circadian oscillator.

The overall mechanism and several components of the circadian oscillator are conserved between mammals and insects. The *Drosophila* genome has only one *Jarid1* family gene, *little*

imaginal discs (*lid*) (fig. S1). Flies carrying the hypomorphic allele *lid*^{10424} (P-element insertion in the first intron) over the balancer chromosome CyO (*lid*^{10424}/*CyO*) expressed less *lid* mRNA than did WT *y;ry* flies (Fig. 3A). Consistent with our observations in *Jarid1a*$^{-/-}$ fibroblasts (Figs. 1 and 2), *lid*^{10424}/*CyO* flies also expressed reduced amounts of *per*, *cry*, and *timeless* (*tim*) mRNA. These *lid*^{10424}/*CyO* flies showed normal activity distribution under a 12 hours of light:12 hours of dark (LD) cycle (Fig. 3B), and their total activity (1030 ± 44, average beam breaks for 3 days in LD, SEM, *n* = 75) was equivalent (*P* > 0.13, one-way ANOVA) to that of WT *y;ry* (831 ± 85, SEM, *n* = 16) or +/*CyO* (938 ± 60 SEM, *n* = 45) flies, which implied no deficit in locomotion or light:dark entrainment of the circadian clock.

However, under constant darkness (DD), the *lid*^{10424}/*CyO* flies exhibited disrupted circadian activity rhythms. The majority of *lid*^{10424}/*CyO* flies showed no or weak circadian activity rhythms (Fig. 3, B and C). Those *lid*^{10424}/*CyO* flies with detectable rhythms showed significant period shortening (Fig. 3C) (*lid*^{10424}/*CyO* = 22.91 ± 0.04 hours;

y;ry = 23.61 ± 0.06 hours; average ± SEM, *n* = 16 and 75; *P* < 0.001). Expression of a genomic copy of *lid* in *lid*^{10424}/*lid*^{10424} homozygous flies (*lid*^{10424}/*lid*^{10424};*gLid*) restored Lid protein expression to near-WT amounts and also restored circadian activity rhythms (Fig. 3C and fig. S11). Furthermore, a demethylase-deficient Lid allele (8) partially rescued the circadian phenotype (*lid*^{10424}/*lid*^{10424};*gJmjC**). Under LD and DD, the *lid*^{10424} flies exhibited attenuated day:night differences in activity. Specifically, the *lid*^{10424} flies exhibited increased activity during midday and reduced dark anticipation (Fig. 3D). Comparable circadian rhythm disruption and reduced expression of CLOCK-BMAL1 (or CYC) targets in both *Drosophila* and mammalian cells supports a conserved role of *lid/Jarid1* in the insect and mammalian circadian oscillator.

In *Jarid1a*$^{-/-}$ mouse fibroblasts, the *Per2* promoter region showed an increased abundance of H3K4me3 (fig. S12A), but a significantly reduced amount of acetylated H3K9 relative to those of WT controls (Fig. 4A). Conversely, overexpression of JARID1a in human embryonic

Fig. 3. Circadian rhythm disruption in *lid*^{10424} flies. (**A**) RT-QPCR of *lid*, *per*, *cry*, and *tim* mRNA in the heads of *y;ry* (black) and *lid*^{10424}/*CyO* (red) flies collected every 4 hours after 72 hours in constant darkness (±SEM, *n* = 3). (**B**) Representative circadian double-plotted actograms of wild-type *lid*$^{+/+}$ (*y;ry*), *lid*^{10424}/*CyO*, *lid*^{10424}/*lid*^{10424};*gLid*, and *lid*^{10424}/*lid*^{10424};*gJmjC** flies under LD or DD conditions. Arrowheads indicate transition from LD to DD. (**C**) (Left) Normalized average activity of *y;ry* (black) and *lid*^{10424}/*CyO* flies (red) (*n* = 33) under LD and DD conditions. (Right) Summary of the circadian activity rhythms in various *Drosophila* strains tested. Histogram shows the percentage of flies with normal (R, rhythmic), weak (W) or no detectable (A, arrhythmic) circadian activity rhythms (+SEM). (**D**) Normalized average activity (+SEM; *n* = 16 to 75) in 30-min bins during the light:dark period show two major phases of activities in *y;ry* flies at morning and evening.
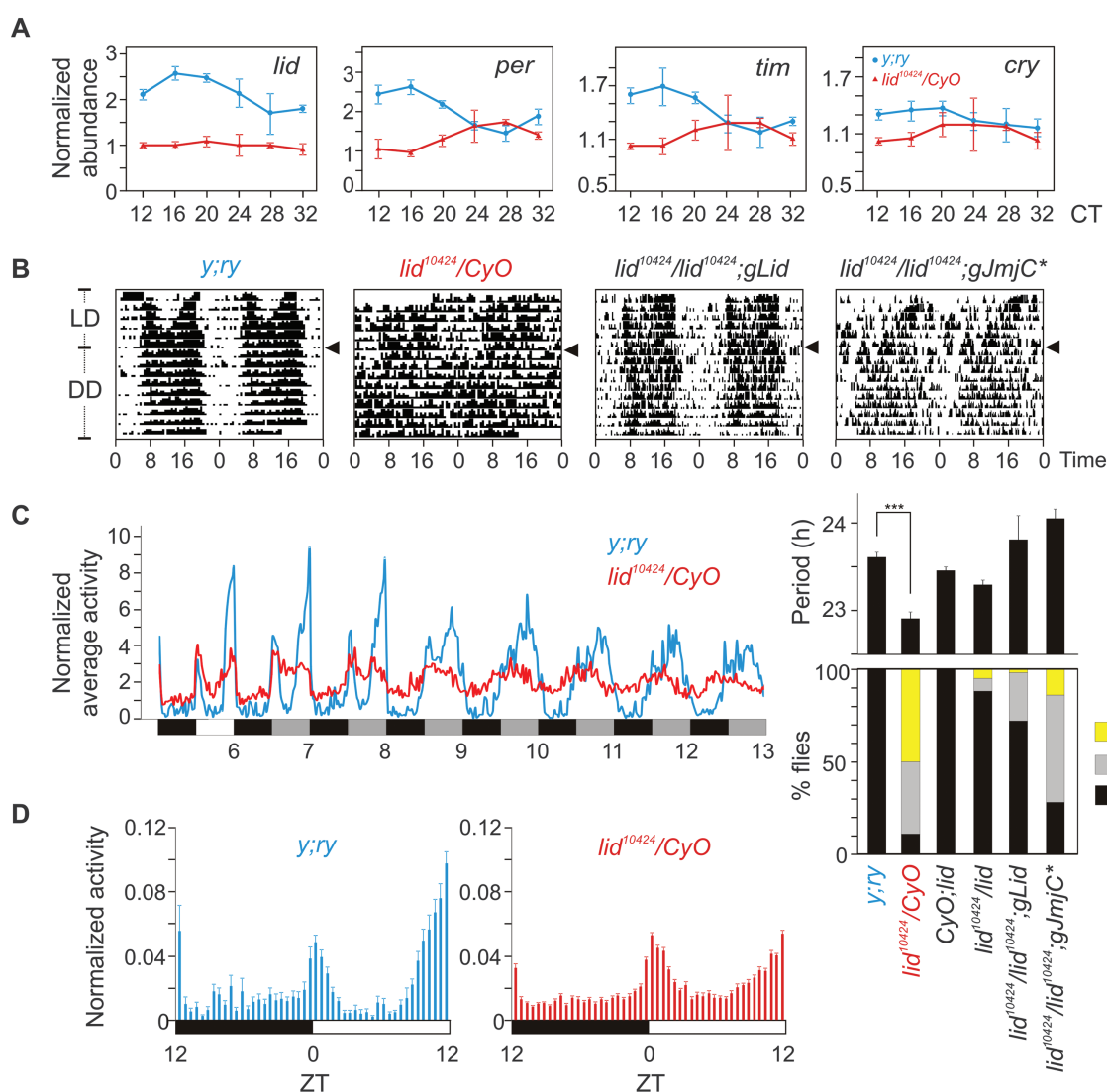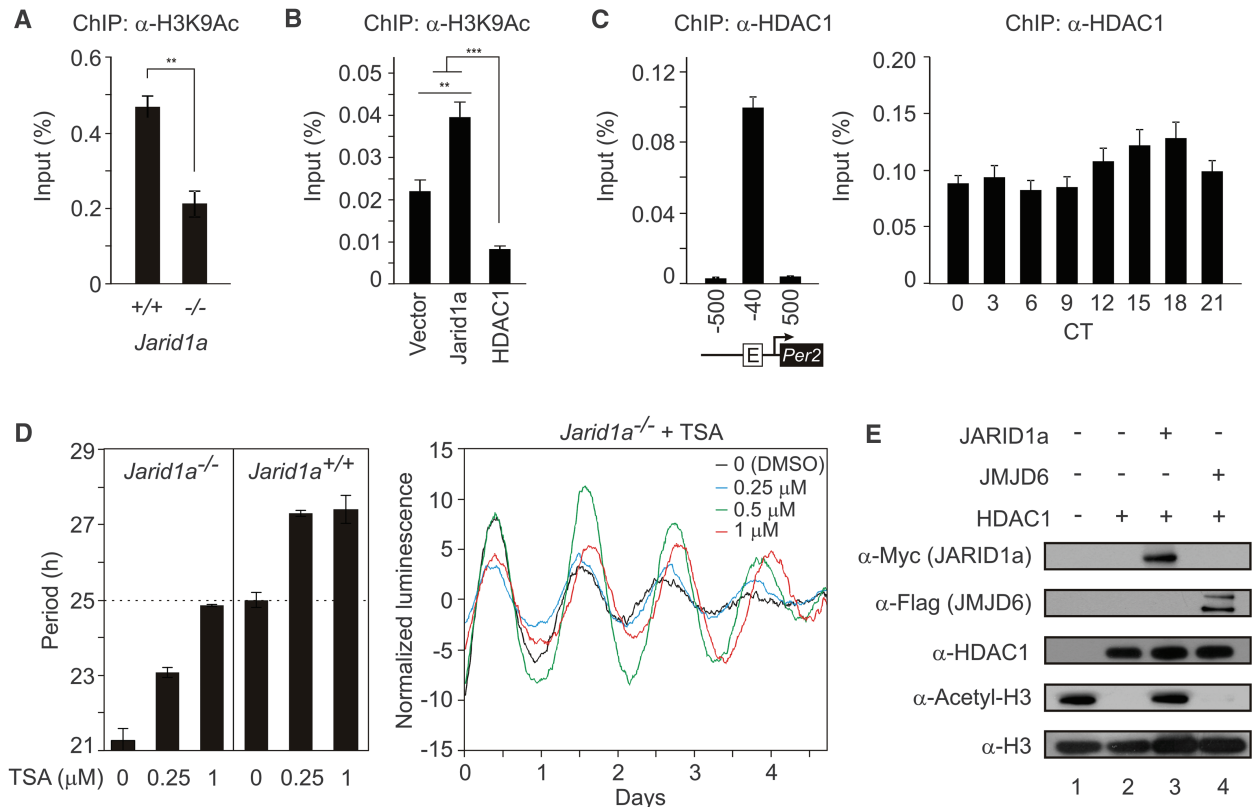
Fig. 4. Dynamic interaction between HDAC and JARID1a correlates with normal histone acetylation at *Per* promoter. (**A**) H3K9Ac detected by ChIP-QPCR in *Jarid1a*$^{-/-}$ or WT cells (average +SEM, n = 3; **P < 0.05). (**B**) H3K9 acetylation at the endogenous *Per2* promoter after overexpression of JARID1a or HDAC1 (**P < 0.001, ***P < 0.0001, n = 3 per group, one-way ANOVA). (**C**) ChIP-QPCR quantification of HDAC1 at E-box of *Per2* promoter in mouse liver. For (A) to (C), chromatin modifications are presented as percent of total chromatin used for immunoprecipitation (% input). (**D**) Effect of various concentrations of TSA on *Per2:Luc* in *Jarid1a*$^{-/-}$ cells . Representative real-time traces are shown. (**E**) Acetylated histone H3 (lane 1) was incubated with 100 ng HDAC1 (lane 2), along with purified JARID1a (lane 3) or JMJD6 (lane 4), and analyzed by immunoblot.

kidney–293 cells (HEK293T cells) increased accumulation of H3K9Ac at the *Per2* promoter (Fig. 4B), but not at a control promoter (fig. S12C). This suggests that coordinated increases in both H3K4me3 and histone acetylation are required for sufficient *Per* induction. Recruitment of JARID1a to *Per* promoters might promote H3K9 acetylation levels during *Per* transcription.

Lid inhibits histone deacetylase Rpd3 to activate transcription at specific loci (*9*). Such HDAC inhibition by Lid, which is independent of its KDM activity, is consistent with the observed activation of CLOCK and BMAL1 by JARID1a (Fig. 1F and figs. S4 and S5). JARID1a also co-immunoprecipitated HDAC1 in mammalian cells (fig. S13). Chromatin immunoprecipitation followed by quantitative PCR (ChIP-QPCR) analysis from mouse liver chromatin showed a nearly constant HDAC1 occupancy at the *Per2* E-box (Fig. 4C). Further, its presence at the *Per2* promoter was unchanged in *Jarid1a*$^{-/-}$ cells (fig. S12B). Although HDAC1 likely mediates repression of *Per2* transcription (*3*) (Fig. 4C and fig. S14), its presence during the activation phase is consistent with enrichment of HDACs at promoters of highly expressed and inducible genes (*5*). The high-amplitude H3K9 acetylation rhythms in the presence of relatively constant amounts of

HDAC1 at the *Per2* promoter could be partly explained by transient inhibition of HDAC activity. Loss of JARID1a might lead to higher HDAC activity during activation phase, low H3K9 acetylation, and reduced *Per* transcriptional activation by CLOCK-BMAL1. Indeed, pharmacological inhibition of HDAC by trichostatin A (TSA) led to increased histone acetylation at the *Per2* promoter, rescued the period-length defect, and improved the amplitude of *Per2:Luc* rhythm in *Jarid1a*$^{-/-}$ cells (Fig. 4D). Similar TSA treatment slightly increased the period length of WT cells, but dampened *Per2:Luc* oscillations (fig. S15). Affinity-purified JARID1a impaired the ability of HDAC1 to deacetylate acetylated histone H3 in vitro, whereas another JmjC domain–containing protein, JMJD6, could not (Fig. 4E and fig. S16).

These results support a model in which JARID1a mediates transition from repression to robust activation of *Per* transcription. During the activation phase, both H3K4me3 and acetylated histones at CLOCK-BMAL1 target sites accumulate in parallel with *Per* transcription. JARID1a appears to be recruited to the *Per* promoter in complex with CLOCK-BMAL1, where it inhibits HDAC1 activity to enhance histone acetylation and transcriptional activation. Although purified JARID1a

or Lid inhibits HDAC activity in vitro, this mode of regulation is likely gene- and context-dependent in vivo. *Jarid1a*$^{-/-}$ cells have increased amounts of H3K4me3 at the *Per* promoter (fig. S12), and overexpression of the JmjC domain of JARID1a slightly repressed *Per* transcription (fig. S5), which suggest that, in vivo, JARID1a may mediate demethylation or that its presence in the transcriptional complex of target genes is required for proper recruitment of other proteins that carry out this function. However, whereas the lysine demethylase activity of JARID1a is dispensable for normal circadian rhythms in mammalian cells, its HDAC-inhibiting function appears to be necessary for proper oscillator function.

References and Notes
1. N. D. Heintzman et al., *Nat. Genet.* **39**, 311 (2007).
2. S. H. Yoo et al., *Proc. Natl. Acad. Sci. U.S.A.* **102**, 2608 (2005).
3. Y. Naruse et al., *Mol. Cell. Biol.* **24**, 6278 (2004).
4. M. Doi, J. Hirayama, P. Sassone-Corsi, *Cell* **125**, 497 (2006).
5. Z. Wang et al., *Cell* **138**, 1019 (2009).
6. S. Katada, P. Sassone-Corsi, *Nat. Struct. Mol. Biol.* **17**, 1414 (2010).
7. R. J. Klose et al., *Cell* **128**, 889 (2007).
8. L. Li, C. Greer, R. N. Eisenman, J. Secombe, *PLoS Genet.* **6**, e1001221 (2010).
9. N. Lee, H. Erdjument-Bromage, P. Tempst, R. S. Jones, Y. Zhang, *Mol. Cell. Biol.* **29**, 1401 (2009).

Superfast Muscles Set Maximum Call Rate in Echolocating Bats

Coen P. H. Elemans,[1]* Andrew F. Mead,[2] Lasse Jakobsen,[1] John M. Ratcliffe[1]*
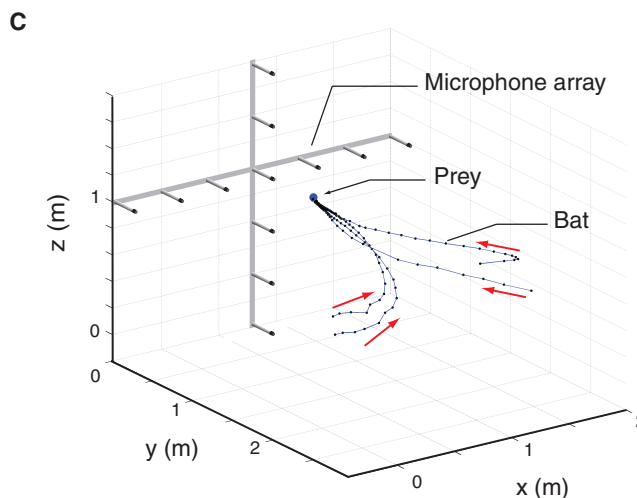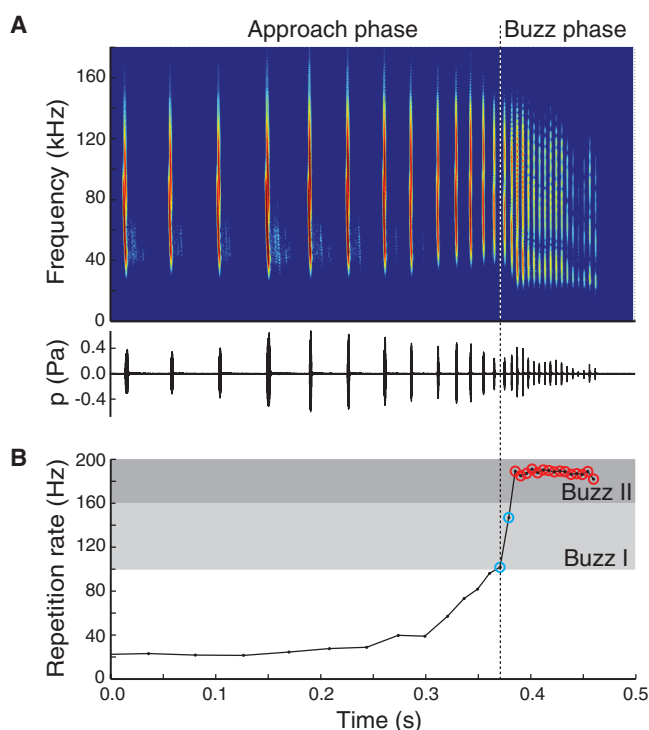
As an echolocating bat closes in on a flying insect, it increases call emission to rates beyond 160 calls per second. This high call rate phase, dubbed the terminal buzz, has proven enigmatic because it is unknown how bats are able to produce calls so quickly. We found that previously unknown and highly specialized superfast muscles power rapid call rates in the terminal buzz. Additionally, we show that laryngeal motor performance, not overlap between call production and the arrival of echoes at the bat's ears, limits maximum call rate. Superfast muscles are rare in vertebrates and always associated with extraordinary motor demands on acoustic communication. We propose that the advantages of rapid auditory updates on prey movement selected for superfast laryngeal muscle in echolocating bats.

Laryngeal echolocation and insectivory characterize about 70% of present-day bat species (1–3). Over the course of an attack on a flying insect, bats increase their echolocation call emission rates as they progress from prey detection, through approach, to the terminal buzz (1, 2, 4) (Fig. 1A). Increasing call emission rates means more information updates per unit time from returning echoes on the relative position of the target. All aerial hawking bats studied to date produce the buzz, which is sometimes subdivided into "buzz I" and "buzz II" phase calls, the former occurring at rates of ~100 to 160 calls/s, and the latter ≥160 calls/s (1, 5) (Fig. 1B). Bats do not call at rates exceeding those reached during this final stage of aerial hawking attack (2, 4), and we hypothesize that call production, echo processing, or both limit maximum echolocation call rate.

Laryngeal nerve-cut experiments reveal that each call a bat emits is under active neuromuscular control (6, 7). Consequently, muscle performance might place an upper limit on the rate at which bats produce calls. Alternatively, if prey echoes overlap with or return after the next call is emitted, accuracy in target ranging may suffer as a result of ambiguity in matching echoes to calls (1, 8). While hunting, most species avoid potential ambiguity by not producing the next call until target echoes reach the bat's ears (1), potentially limiting maximum call rates during the buzz. To investigate these hypotheses, we first measured sound production during aerial attack sequences in free-flying Daubenton's bats (*Myotis daubentonii*, Vespertilionidae) using a 12-microphone array (Fig. 1C) (9) and determined when the start and the end of each prey echo (Fig. 2, A to C) would impinge upon the bat's ears relative to both the source call and the next call emitted (10). Our data show that during a buzz, echoes from individual calls terminate before the start of the next call (Fig. 2C and fig. S1), suggesting no ambiguity in call-echo matching. In fact, for buzz II calls, the repetition rate could theoretically exceed 400 calls/s without any such ambiguity (Fig. 2C and fig. S1), a rate twice as high as the 190 calls/s observed in our study (Fig. 1). Our results also demonstrate that, because call duration decreases during the buzz, there is no overlap between a call and its echo until the bat is less than 5 cm from its target (Fig. 2B), corroborating previous estimates for

[1]Institute of Biology, University of Southern Denmark, DK-5230 Odense M, Denmark. [2]Department of Biology, University of Pennsylvania, Philadelphia, PA 19104, USA.

*To whom correspondence should be addressed. E-mail: coen@biology.sdu.dk (C.P.H.E.); jmr@biology.sdu.dk (J.M.R.)

Fig. 1. Echolocation and flight kinematics during aerial attack sequences in *Myotis daubentonii*. (**A**) Spectrogram and oscillogram of emitted echolocation calls as recorded on the center microphone of the array. (**B**) Instantaneous call repetition rates from sequence in (A). The start of buzz I is defined as call repetition rate >100 calls/s (cyan circles, light gray zone). In buzz II, the repetition rate is >160 calls/s (red circles, medium gray zone); here, peak fundamental frequency of the calls drops from 45 to 25 kHz. (**C**) Four reconstructed flight paths from a single bat using a 12-microphone array (10). Red arrows indicate flight direction.